

Vibration Monitoring of the Rock Formation Above the Hatshepsut Temple

Alexander MENDLER¹, Juan D. RADA ERAZO¹, Mohamed ISMAEL^{2,5},
Mostafa EZZY^{2,5}, Benjamin JACOBS³, Christian HABERLAND⁴,
Michael KRAUTBLATTER³, Hany HELAL^{2,5}, Christian U. GROSSE¹

¹ Technical University of Munich, TUM School of Engineering and Design,

Dept. of Materials Engineering, Chair of Non-destructive Testing, Munich, Germany

² Department of Mining, Petroleum, and Metallurgical Engineering, Faculty of Engineering, Cairo University, Giza, Egypt

³ Technical University of Munich, TUM School of Engineering and Design, Dept. of Civil and Environmental
Engineering, Chair of Landslide Research, Munich, Germany

⁴ Helmholtz Centre Potsdam, German Research Centre for Geosciences, Potsdam, Germany

⁵ Unesco Chair on 'Science and Technology for Cultural Heritage', Faculty of Engineering, Cairo University, Giza, Egypt

Abstract. The Hatshepsut temple in Egypt is a masterpiece of ancient architecture. Just as distinct as the temple itself is the rock formation it is carved into, and recurring rock falls in the vicinity have raised concerns regarding the temple's safety under progressing erosion and seismic activity. Due to the material characteristics (brittle carbonate rock), high gravitational stresses could lead to rapid crack propagation, and vibration-based measures may be suitable precursors for imminent rock falls. This paper describes a one-day measurement campaign on the rock towers above the temple as a preliminary study prior to the implementation of a long-term seismic station. Next to operational modal analysis, horizontal-to-vertical spectral ratios are evaluated to cross-validate the resonance behaviour. Stochastic subspace identification (SSI) is applied for the estimation and automated tracking of natural frequencies and damping ratios of the rock tower. One of the advantages of the applied method is the inherent uncertainty quantification, meaning for each vibration record, the mean values and the standard deviations are estimated for each modal parameter, giving deep insights into the reliability of the vibration-based monitoring of rock formations.

Keywords: Vibration-based monitoring, stochastic subspace identification, horizontal-to-vertical spectral ratios, environmental and operational variables.

Introduction

The ambient vibrations of soil and rock formations carry valuable information on the dynamic behaviour. They can be analysed to determine the fundamental resonance frequencies, and thus, classify the soil based on national standards. They also carry information on the seismic



response, the local site amplification, and the local energy dissipating mechanism. Moreover, the directivity of predominant motion can be determined, which aids in the prediction of failure modes of rock towers, rock arches, or rock slopes. Dynamic properties, such as the resonance frequencies, are often used for the model updating of numerical models [1,2,3,4]. Moreover, the coupling behaviour of different rock faces can be analysed [5] as well as environmental effects, such as temperature or water saturation [6]. Material changes often lead to changes in the resonance frequencies or damping ratio, and therefore, frequency monitoring is an appropriate technique for early warning systems [7].

Various methods exist to estimate the resonance frequencies. In geotechnical engineering, the standard spectral ratio (SSR) is often used to characterize soil based on a reference sensor on bedrock and a second sensor on the site of interest. If the measurement is performed based on a single sensor station, the horizontal-to-vertical spectral ratios (HVSRs) can be applied [8], as demonstrated by Lermo and Chavez-Garcia [9]. Increasingly, modal analysis techniques are adopted from civil engineering, as they can determine multiple resonance frequencies, modal damping ratios, and mode shapes. Where damping ratios describe the energy dissipation characteristics, mode shapes describe the directivity of motion. Geimer et al. [6], for example, applied the peak picking method to estimate the (damped) natural frequency of a natural rock arch. Glueer et al. [1] employed the frequency domain decomposition (FDD) to analyse the rock slopes surrounding an alpine ammunition storage facility. The enhanced FDD has been applied to estimate the modal properties of rock towers [10], sediment-filled layers [11], and rock slopes [12]. Häusler et al. [13] demonstrated that the half-power bandwidth method and the logarithmic decrement technique yield reliable damping estimates for natural rock arches. Although subspace system identification (SSI) [14] is one of the most powerful modal analysis techniques, they are rarely applied in geotechnical applications. Reynders [15] showed that it is more accurate and precise than the FDD or other output-only modal analysis methods. It can cope with weakly excited and closely spaced modes. Various subversions exist to correlate ambient measurements (covariance-driven vs. data-driven) and to weight the resulting block Hankel matrices, e.g., the principle component algorithms, unweighted principal components algorithm, and canonical variate algorithm [14]. State-of-the-art versions can estimate the uncertainties in all modal parameters based on a single measurement record [16,17]. Some studies have applied SSI for the assessment of soil layers and rock formations, for example, Soltani et al. [18] and Häusler et al. [13], but the uncertainty quantification is often neglected. Estimating the uncertainty (the estimation error) is particularly important for damping ratios, as they are highly scattered quantities. Moreover, uncertainty estimation is key for a reliable damage diagnosis based on the Mahalanobis distance and other anomaly detection tests that are implemented in early warning systems.

This paper applies SSI for the rock monitoring at the Hatshepsut temple. Special focus is put on the uncertainty quantification of natural frequencies, damping ratios, and mode shapes. Furthermore, the SSI stabilizing diagram is combined with the HVSRs for the first time in order to display information on the site amplification and modal parameters in one single chart. The remainder of the paper is organized as follows: Section 1 introduces the considered case study of a rock tower behind the Hatshepsut temple in Egypt. Section 2 recaps the HVSR and the SSI method, and explains how the results can be combined in one chart. In Section 3, the results from monitoring the Hatshepsut rock needle are presented, followed by some conclusions in Section 4.

1. Case Study

The Hatshepsut temple is a masterpiece of ancient architecture from the 15th century B.C. It is located close to the city of Luxor in Egypt. Just as distinct as the temple itself is the rock formation it is carved into, with hanging cliffs and distinct rock towers, see Fig. 1. In this paper, a one-day measurement campaign is conducted. The goal of this preliminary study is to understand the vibration behaviour of the rock tower before a long-term seismic station can be implemented as part of an early warning system. Recurring rock falls in the vicinity have raised concerns regarding the temple's safety under progressing erosion and seismic activity. The cliff is composed of Thebes limestone and Esna Shale formations at its base, which is susceptible to water-induced expansion in case of rainfall and flash floods. Due to the material characteristics (brittle carbonate rock), high gravitational stresses could lead to rapid crack propagation, and vibration-based measures may be suitable precursors for rock falls.



Fig. 1. Rock tower above the Hatshepsut temple and aerial view of sensor location

During the measurement campaign, a Nanometrics Trillium Compact 120 s seismometer was placed at the top of the rock tower together with a CUBE and Breakout Box data acquisition system, and an autonomous power supply. All signal processing parameters are summarized in Table 1. The broadband vibration sensor was levelled and oriented north.

Table 1. Signal processing parameters

	Acquisition date	Duration	Sampling frequency
Seismometer TC 120 s	March 6 th 2023	09:37 to 23:43	200 Hz

2. Methods

This section summarizes the signal processing methods applied to the seismometer measurements. Next to the HVSR, the SSI method is applied to estimate natural frequencies and damping ratios. Ultimately, an approach is proposed that summarizes the results from both methods in a single chart.

2.1 HVSR

The *horizontal-to-vertical spectral ratio (HVSR)* is a frequency domain-based method to determine the resonant frequency of soil based on a single tri-axial sensor [8,19,20]. It is defined as

$$HVSR = \frac{|H_S|}{|V_S|}, \quad (1)$$

where H_V is the spectral densities of the vertical channels, V_S is the spectral density of the merged horizontal components, and $|\cdot|$ is the absolute value operator. Since the directivity of the vibrations is unknown a priori, both horizontal channels are Fourier-transformed, and merged using the geometric mean [21]. For bedrock, the HVSR is equal to one over the entire frequency spectrum, and a HVSR beyond one quantifies the site amplification for certain frequencies, see Fig. 2 (left). The figure shows a representative mean curve and the 95% confidence intervals for uncertainty quantification. The method was originally designed for flat and homogenous soil layers, and assumes that the vertical vibration components are not amplified within the soil. The algorithm critically depends on the frequency resolution, i.e., the number of data points for the Fourier transformation. Stationary vibrations are assumed, and STA/LTA triggers [22] are implemented to remove records with transient events.

2.2 SSI

Stochastic subspace identification (SSI) is a time-domain based method to determine modal frequencies, damping ratios, and mode shapes [14]. The main idea is to fit a stochastic state space model to the vibration data using regression techniques

$$\begin{aligned} \mathbf{x}_{k+1} &= \mathbf{A}\mathbf{x}_k + \mathbf{w}_k \\ \mathbf{y}_k &= \mathbf{C}\mathbf{x}_k + \mathbf{v}_k, \end{aligned} \quad (2)$$

where \mathbf{x}_{k+1} and \mathbf{y}_k are the state vector and the measurement vector, and \mathbf{A} and \mathbf{C} are the state transition and the output matrix. The terms \mathbf{w}_k and \mathbf{v}_k describe process noise and measurement noise. Subsequently, the eigenvalue problem of the vibration model from Eq. (2) is solved $\mathbf{A} = \mathbf{\Phi}\mathbf{\Lambda}\mathbf{\Phi}^{-1}$ with $\mathbf{\Lambda} = \text{diag}(\mathbf{z})$ to obtain the eigenvalues \mathbf{z} and the eigenvectors in $\mathbf{\Phi}$. The poles are translated into the natural frequency $f_n = \omega_n/(2\pi)$ and modal damping ratio ζ_n of each mode of vibration $n = 1 \dots m$, or the damped natural frequency $f_{d,n}$,

$$\mu_n = \frac{\ln z_n}{\Delta t} = \omega_n \zeta_n \pm \omega_n \sqrt{1 - \zeta_n^2} i \quad (3)$$

$$f_n = \frac{|\mu_n|}{2\pi}, \quad \zeta_n = -\frac{\text{Re}(\mu_n)}{|\mu_n|}, \quad f_{d,n} = f_n \sqrt{1 - \zeta_n^2}, \quad (4)$$

where Δt is the time between two samples, i is the imaginary unit, and $Re(\cdot)$ denotes the real part of the pole μ_n . The algorithm requires the number of modes m to be set by the user. Since this value is unknown, the mode estimation is repeated for a user-defined range of model orders. Next, the model order of each solution is plotted against the frequencies in so-called stabilization diagrams, see Fig. 2 (centre). What follows is an iterative process of clustering the vertical frequency lines and statistically merging all solutions within one cluster [23]. For uncertainty quantification, perturbation-based approaches can be applied to a single measurement record to quantify the uncertainties in the measurements, propagate them through the modal analysis procedure, and project them onto the natural frequencies and damping ratios [16,17]. Typically, the estimation accuracy is displayed through error bars with a magnitude equal to one standard deviation, see Fig. 2 (centre). The most important user input parameters are the number of time lags used for the estimation of covariance functions as well as the model order.

2.3 Combined HVSR and SSI

In previous sections, the HVSR and the SSI are reviewed, and this section proposes an approach that combines the results from both methods in one chart, see Fig. 2 (right). The HVSR describes the amplification of ground motions at different frequencies. Moreover, the fundamental frequencies can be extracted from HVSR curves as the x-values of the largest peaks [21]. The SSI method, on the other hand, can estimate multiple natural frequencies over a wide frequency range. Moreover, damping ratios and mode shapes are estimated simultaneously, which describe the energy dissipating characteristics of the examined structure and the directivity of motion at different natural frequencies, respectively. Through optimized parameter settings, weakly excited modes can be estimated reliably, even if they do not form peaks in the Fourier transform or the HVSR. It is a time domain method, meaning the signal is not transferred into the frequency domain and the frequency resolution does not affect the results. New users often perceive SSI as a black box due to the limited visualization capabilities, and that is why the stabilizing diagram from Fig. 2 (centre) is often plotted together with the power spectral density in one plot, or the singular values of the power spectral density matrix. In this paper, SSI-based stabilizing diagrams are combined with HVSR, see Fig. 2 (right). This helps the operator with interpreting the stabilizing diagrams. If a vertical line forms underneath a peak in the HVSR curve, this peak likely describes resonance phenomena and if a vertical line forms in a flat frequency spectrum, the HVSR most likely missed some important amplification effects. Therefore, the results are synergetic and the methods can be used for cross-validation.

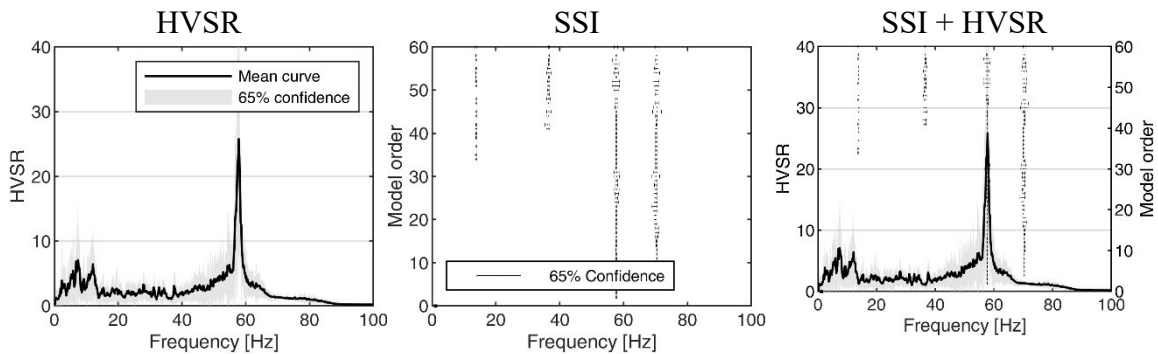


Fig. 2. HVSR with 65% confidence interval (left), SSI stabilizing diagram with error bars for the 65% confidence interval (centre), and combined HVSR and SSI (right)

3. Results and Discussion

In this section, the SSI and HVSR methods are applied to vibration data measured on the rock tower behind the Hatshepsut temple, see Fig. 1. First, a single representative measurement record is evaluated to demonstrate the advantages of the combined SSI and HVSR chart and to assess the quality of the HVSR estimates. Subsequently, the modal parameters are tracked over the course of one day to demonstrate the suitability of damping ratios as damage indicators, and ultimately, each section contains a critical discussion.

3.1 Short-term Tests

The results of the short-term test are summarized in Fig. 2. The record duration is set to 5 min in accordance with international guidelines [21]. The HVSR, shown in the left subplot, exhibits a distinct peak at 57.81 Hz, indicating that the ground motion amplification at the tip of the rock tower is the strongest at this frequency. SSI identified four peaks at 13.8 Hz, 36.59 Hz, 57.72 Hz and 70.29 Hz. Both methods identified the resonance frequency at 57.72 Hz, which cross-validates the results. However, the SSI method does not depend on the frequency resolution (1,024 frequency lines) and it yields the standard deviation as well, see Table 2. Typically, the measurement error is quantified after repeatedly estimating the modal parameters, but the perturbation-based approach applied in this paper [16,17] enables an uncertainty quantification based on a single measurement record. This significantly increases the reliability of any statement that is deduced from natural frequency and damping ratio estimates.

Table 2. Resonant frequencies and damping ratios of the Hatshepsut rock tower

	Mode 1	Mode 2	Mode 3	Mode 4
HVSR			57.81 Hz	
SSI	13.80 ± 0.04 Hz 1.15 ± 0.32 %	36.59 ± 0.07 Hz 0.82 ± 0.20 %	57.72 ± 0.08 Hz 1.24 ± 0.09 %	70.29 ± 0.08 Hz 1.69 ± 0.18 %

In addition to natural frequencies, the SSI yields the modal damping ratios from Table 2 and the mode shapes shown in Fig. 4, together with their standard deviation. Mode shapes are complex-valued but the figure only shows the real parts. They reveal the directivity of motion but they should not be mistaken for absolute vibration amplitudes. That is why they are normalized to unit displacement for visualization. Mode 1 and 3 primarily oscillate along the cliff face where Mode 4 vibrates perpendicular to it and toward the temple. The directivity of Mode 2 is harder to interpret as it contains components along and perpendicular to the rock face. Moreover, it exhibits the highest estimation uncertainties, indicated by the large grey area that corresponds to the 65% confidence interval. Probably, it is a rotational mode of vibration, and the sensor is not perfectly placed in the centre of the rock tower.

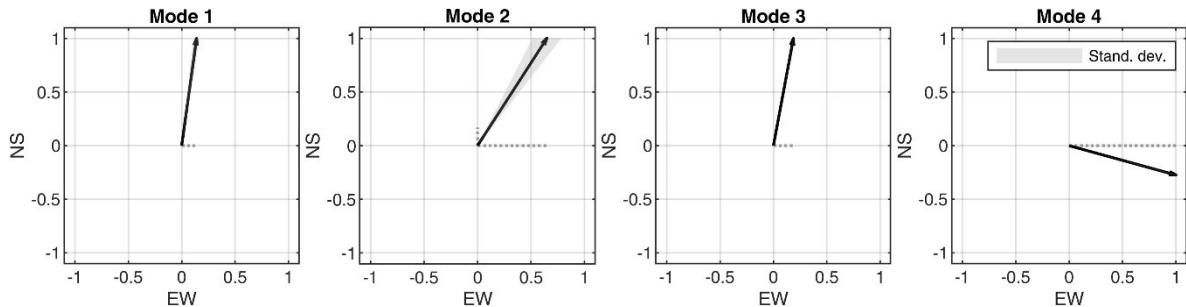


Fig. 3. SSI-based mode shape estimates indicate the directivity of motion at natural frequencies

Based on experience with tower structures, the first mode of vibration at 13.8 Hz exhibits the highest vibration amplitudes at the tip of the rock (the sensor location), as the tower behaves like a vertical cantilever beam. During an earthquake, the first mode of vibration will likely be excited strongly, and may significantly contribute to the observed failure modes. Higher-frequency peaks correspond to modes of vibration that do not exhibit the maximum vibration amplitudes at the tip of the needle but are closer to its base. These modes typically exhibit lower vibration amplitudes and are excited less strongly. Minor peaks can be recognized in the HVSR at 7.42 Hz and 12.11 Hz, but the uncertainties are high (quantified through a wide confidence interval) and do not fulfil the clarity criteria for HVSR [21], so they would have to be discarded. Consequently, the most critical modes of vibration would have been missed using HVSR alone, which underlines the advantages of the combined HVSR and SSI chart. The authors are aware that the sensor location may violate the free-field assumption made in the derivation of the HVSR. Nonetheless, this study points out that SSI leads to much more comprehensive and reliable results than HVSR, as it yields damping ratios and mode shapes as well as the associated measurement errors. One may argue that the HVSR describes the amplification behaviour over the entire frequency spectrum, which the SSI does not. However, various studies have shown that the amplification factors can vary significantly between different estimation methods [24,25,26,27]. To conclude, SSI is a powerful method that may replace HVSR in the long term for the estimation of fundamental frequencies of soil and rock formations based on a single measurement station.

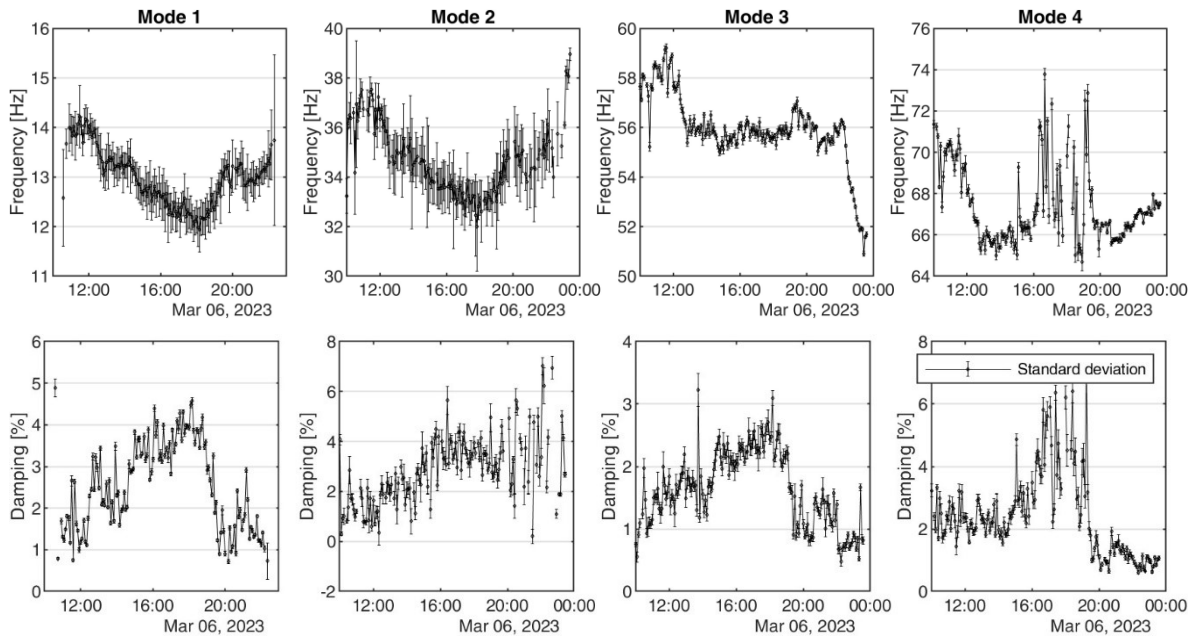


Fig. 4. SSI-based natural frequency and damping estimates

3.2 Long-term Monitoring

In the following, the SSI-based natural frequencies and damping ratios are tracked over the course of half a day, see Fig. 4 and Table 1. The figure not only shows the estimated frequencies and damping ratios but also their measurement error through vertical error bars, with a magnitude of one standard deviation. The first two frequencies vary between 12.0 Hz and 14.5 Hz and show a strong negative correlation with ambient temperature readings. The highest temperatures are measured around 15:00 and the lowest frequencies three hours later (around 18:00). The delay could be explained by the gradual warming up of the rock tower. The damping ratios, on the other hand, are positively correlated with temperature changes (meaning high temperature leads to high damping ratios) and show a stronger fluctuation

over the course of one day with mean values between 1.5% and 4.5%. Vibration-based features that are sensitive to environmental change are also sensitive to changes in the structural and material properties [28], so they might be appropriate damage indicators for an early warning system at the examined site.

4. Conclusion

This paper applies two vibration-based methods to the seismometer data from the Hatshepsut rock tower in Egypt, that is, the horizontal-to-vertical spectral ratio (HVSR) and an operational modal analysis method called stochastic subspace identification (SSI). For the first time, the results from the HVSR and combined with the SSI stabilizing diagram in one chart, cf. Fig. 2. To the author's knowledge, this is the first case study, where SSI is applied to a rock formation in combination with a perturbation-based approach for uncertainty quantification that enables the estimation of the measurement error for natural frequency and damping estimates based on a single measurement record. This way, modal frequencies, damping ratios, and mode shapes can be evaluated together with ground amplification factors based on a single sensor station with three vibration channels. Other modal analysis methods, such as the FDD, require more than one sensor [29]. This is not the case for SSI, and therefore, the developed single-sensor approach is the most comprehensive and most reliable method, as it also yields the uncertainties in modal estimates.

Acknowledgements

Special thanks go to the Geophysical Instrument Pool Potsdam (GIPP) at Helmholtz Centre Potsdam GFZ, German Research Centre for Geosciences, Germany, for providing the measurement equipment for this study. Moreover, we would like to thank the Faculty of Engineering at Cairo University for allowing us to record and publish the results in the scope of the HERITAGE project. Our gratitude is extended to Unesco Chair on 'Science and Technology for Cultural Heritage', Faculty of Engineering, Cairo University as well as Supreme Council of Antiquities, Ministry of Tourism and Antiquities for their support.

References

- [1] Glueer, F., Häusler, M., Gischig, V., & Fäh, D. (2021). *Coseismic stability assessment of a damaged underground ammunition storage chamber through ambient vibration recordings and numerical modelling*. *Frontiers in Earth Science*, 9, 773155.
- [2] Moore, J. R., Geimer, P. R., Finnegan, R., & Bodtker, J. (2020). *Between a beam and catenary: Influence of geometry on gravitational stresses and stability of natural rock arches*. *Geomorphology*, 364, 107244.
- [3] Moore, J. R., Geimer, P. R., Finnegan, R., & Thorne, M. S. (2018). *Use of seismic resonance measurements to determine the elastic modulus of freestanding rock masses*. *Rock Mechanics and Rock Engineering*, 51, 3937-3944.
- [4] Wang, M., Chi, S., & Liu, Z. (2023). *Dynamic Parameters Updating of Earth-rock Dams Based on Modal Parameter Identification*. *KSCE Journal of Civil Engineering*, 27(10), 4163-4175.
- [5] Dietze, M., Krautblatter, M., Illien, L., & Hovius, N. (2021). *Seismic constraints on rock damaging related to a failing mountain peak: the Hochvogel, Allgäu*. *Earth Surface Processes and Landforms*, 46(2), 417-429.
- [6] Geimer, P. R., Finnegan, R., & Moore, J. R. (2022). *Meteorological controls on reversible resonance changes in natural rock arches*. *Journal of Geophysical Research: Earth Surface*, 127(10), e2022JF006734.

- [7] Lévy, C., Baillet, L., Jongmans, D., Mourot, P., & Hantz, D. (2010). *Dynamic response of the Chamousset rock column (Western Alps, France)*. Journal of Geophysical Research: Earth Surface, 115(F4).
- [8] Nakamura Y., 1989. *A method for dynamic characteristics estimation of subsurface using microtremor on the ground surface*. Quaterly Report Railway Tech. Res. Inst., 30-1, 25-30.
- [9] Lermo, J., & Chávez-García, F. J. (1994). *Are microtremors useful in site response evaluation?* Bulletin of the seismological society of America, 84(5), 1350-1364.
- [10] Moore, J. R., Geimer, P. R., Finnegan, R., & Michel, C. (2019). *Dynamic analysis of a large freestanding rock tower (Castleton Tower, Utah)*. Bulletin of the Seismological Society of America, 109(5), 2125-2131.
- [11] Poggi, V., Ermert, L., Burjanek, J., Michel, C., & Fäh, D. (2014). *Modal analysis of 2-D sedimentary basin from frequency domain decomposition of ambient vibration array recordings*. Geophysical Journal International, 200(1), 615-626.
- [12] Häusler, M., Michel, C., Burjánek, J., & Fäh, D. (2019). *Fracture network imaging on rock slope instabilities using resonance mode analysis*. Geophysical Research Letters, 46(12), 6497-6506.
- [13] Häusler, M., Geimer, P. R., Finnegan, R., Fäh, D., & Moore, J. R. (2021). *An update on techniques to assess normal-mode behavior of rock arches by ambient vibrations*. Earth Surface Dynamics, 9(6), 1441-1457.
- [14] van Overschee, P. and de Moor, B. (1995). *Subspace identification for linear systems: Theory-Implementation-Application*. Kluwer Academic Publishers, Boston/London/Dordrecht.
- [15] Reynders, E. (2012). *System identification methods for (operational) modal analysis: review and comparison*. Archives of Computational Methods in Engineering, 19, 51-124.
- [16] Reynders, E., Pintelon, R., & De Roeck, G. (2008). *Uncertainty bounds on modal parameters obtained from stochastic subspace identification*. Mechanical Systems and Signal Processing, 22(4), 948-969.
- [17] Döhler, M., & Mevel, L. (2013). *Efficient multi-order uncertainty computation for stochastic subspace identification*. Mechanical Systems and Signal Processing, 38(2), 346-366.
- [18] Soltani, H., Muraleetharan, K. K., & Runolfsson, T. (2016). *Modal identification of a centrifuge soil model using subspace state space method*. Soil Dynamics and Earthquake Engineering, 88, 280-296.
- [19] Nogoshi M. and T. Igarashi, 1971. *On the amplitude characteristics of microtremor (Part 2)* (in Japanese with English abstract). Journal of the Seismological Society of Japan, 24(1), 26-40.
- [20] Kanai K. and T. Tanaka, 1961. *On microtremors*. VIII. Bulletin of the Earthquake Research Institute, 39- 97-114.
- [21] Acerra, C., Aguacil, G., Anastasiadis, A., Atakan, K., Azzara, R., Bard, P. Y., ... & Zacharopoulos, S. (2004). *Guidelines for the implementation of the H/V spectral ratio technique on ambient vibrations measurements, processing and interpretation*. European Commission–EVG1-CT-2000-00026 SESAME.
- [22] Withers, M., Aster, R., Young, C., Beiriger, J., Harris, M., Moore, S., & Trujillo, J. (1998). *A comparison of select trigger algorithms for automated global seismic phase and event detection*. Bulletin of the Seismological Society of America, 88(1), 95-106.
- [23] Döhler, M., Andersen, P., & Mevel, L. (2017, May). *Variance computation of modal parameter estimates from UPC subspace identification*. In IOMAC-7th International Operational Modal Analysis Conference, Ingolstadt, Germany.
- [24] Field, E. H., & Jacob, K. H. (1995). *A comparison and test of various site-response estimation techniques, including three that are not reference-site dependent*. Bulletin of the seismological society of America, 85(4), 1127-1143.
- [25] Bonilla, L. F., Steidl, J. H., Lindley, G. T., Tumarkin, A. G., & Archuleta, R. J. (1997). *Site amplification in the San Fernando Valley, California: variability of site-effect estimation using the S-wave, coda, and H/V methods*. Bulletin of the Seismological Society of America, 87(3), 710-730.
- [26] Riepl, J., Bard, P. Y., Hatzfeld, D., Papaioannou, C., & Nechtschein, S. (1998). *Detailed evaluation of site-response estimation methods across and along the sedimentary valley of Volvi (EURO-SEISTEST)*. Bulletin of the Seismological Society of America, 88(2), 488-502.
- [27] Parolai, S., Bindi, D., & Augliera, P. (2000). *Application of the generalized inversion technique (GIT) to a microzonation study: numerical simulations and comparison with different site-estimation techniques*. Bulletin of the Seismological Society of America, 90(2), 286-297.
- [28] Farrar, C. R., & Worden, K. (2012). *Structural health monitoring: a machine learning perspective*. John Wiley & Sons, Wiley, Oxford, United Kingdom.
- [29] Brincker, R., & Ventura, C. (2015). *Introduction to operational modal analysis*. John Wiley & Sons. Chichester, United Kingdom.